SPRFMO

**5th Meeting of the Scientific Committee**

Shanghai, China, 23 - 28 September 2017

# SC5-SQ03

Spatial difference in elemental signatures within early ontogenetic statolith for identifying Jumbo flying squid natal origins

*Bilin Liu, Xinjun Chen & Gang Li*

# Spatial difference in elemental signatures within early ontogenetic statolith for identifying Jumbo flying squid natal origins

Bilin Liu, Xinjun Chen, Gang Li

National Data Center for Distant-water Fisheries, Shanghai Ocean University

## 1. INTRODUCTION

*Dosidicus gigas* (d'Orbigny, 1835), commonly known as the Humboldt or Jumbo (flying) squid, is an eastern Pacific nerito-oceanic species distributed along the eastern coast of the Americas from Alaska to Chile and inhabiting from the sea surface down to a depth of 1200 m (Nigmatullin *et al*. 2001). The abundance of this species tends to be closely related to both environmental conditions (e.g., temperature and predator abundance) and spawner-recruitment dynamics (Waluda *et al*. 2006; Zeidberg and Robsin 2007; Keyl *et al*. 2008). *Dosidicus gigas* is a key species in pelagic ecosystems because of its high abundance and important role in trophic dynamics (Rosas-Luis *et al* 2008). This squid species supports important fisheries in four areas: the Gulf of California (Nevárez-Martínez *et al*. 2000; Morales-Bojórquez *et al*. 2001), the region of the Costa Rica Dome (Ichii *et al*. 2002), the coastal and oceanic waters of Peru (Taipe *et al*. 2001; Waluda *et al*. 2004a; Chen and Zhao 2006) and within and outside the Chilean Exclusive Economic Zones (EEZ) (Rocha and Vega 2003; Zúñiga *et al*. 2008; Liu *et al*. 2010).

The intra-specific population structure of *D. gigas* is complicated. Three groups have been identified based on the size of adult females and males (Nigmatullin *et al*. 2001): a small-sized group (140-340 mm and 130-260mm for females and males respectively) occurring mainly in the equatorial waters; a medium-sized group (280-600 mm and 240-420mm, for females and males respectively) distributed over the whole range of the species; and a large-sized group (550- 650 to 1000-1200 mm

and >400-500mm, for females and males respectively) only inhabiting the northern and southern extremes of its ranges. However, other studies have grouped *D. gigas* into just two stocks being the 'northern' and 'southern' stocks based on their migration patterns (Nesis 1983; Clarke and Paliza 2000; Sandoval-Castellanos *et al.* 2007).

Understanding the population structure and connectivity of marine organisms is critical for studying their population dynamics and developing effective conservation and sustainable management strategies (Thorrold *et al.* 2001; Gillanders 2002). Recently natural geochemical signatures of trace elements and isotopes in the hard structures of marine animals, such as bivalve shells, fish otoliths, octopus styles and squid beaks and statoliths, have been successfully utilized to investigate the population distribution of animals (Campana 1999; Ikeda *et al.* 2003; Becker *et al.* 2005; Cherel and Hobson 2005; Doubleday *et al.* 2008). Elemental signature is considered to be a potential complement to more commonly used genetic and morphologic methods for defining cephalopod cohorts and population structures (Arkhipkin 2005). The hard parts of organisms formed in the early ontogenetic stages potentially carry natural tags recording the environmental history experienced at or near the place where they were born (Campana 1999; Thorrold *et al.* 2001). Thus, elemental signatures in invertebrate larval statoliths are considered as useful tags of natal source (Zacherl *et al.* 2003; Zacherl 2005). For example, Ba/Ca was generally considered as an indicator element for upwelling events, thus the population with higher Ba/Ca value always experience strong upwelling water mass (Arkhipkin et al. 2004; Zumholz et al. 2007). Signatures in the pre-hatching region of the adult otolith can be used to identify the source of populations because they are shown to match with signatures from equivalent structures from juveniles (Forrester and Swear 2002; Hamer *et al.* 2005). The same is found in the statoliths of squid (Warner *et al.* 2009).

During the late 1990s and early 2000s, Proton induced X-ray emission (PIXE) and Electron microprobe analysis (EPMA) were commonly used to examine cephalopod statolith micro-chemistry (Durholtz *et al.* 1997; Yatsu *et al.* 1998; Ikeda

*et al* 2002, 2003). However, these studies focused on Sr, the most abundant element incorporated into the aragonite matrix of statoliths. Recently, laser ablation inductively coupled plasma mass spectrometry (LA-ICP-MS) has become increasingly popular for examining lower concentration trace elements like Ba, Mg and Mn (Zumholz *et al*. 2006, 2007; Doubleday *et al*. 2008; Warner *et al*. 2009; Liu *et al*. 2011).

In this study, we used LA-ICP-MS to determine the elemental signatures in statoliths nuclear (N), representing the embryonic stage, and postnuclear (PN), representing the paralarval stage, of *D. gigas* off the EEZs in the Eastern Pacific Ocean (Arkhipkin 2005). The objectives of this paper are to detect the elemental composition in N and PN of adult statoliths, to determine if elemental signatures differ among different geographic groups, to determine the validity of using elemental signatures in discriminating populations, and to identify the most suitable part of a statolith for population identification. This study provides an alternative way to evaluate the *D. gigas* population structure on the three major fishing grounds, which can improve our knowledge of population connectivity, natal origins and life history for fisheries management.

## 2. MATERIALS AND METHODS

### *Sampling*

A total of 59 specimens were sampled in Chinese scientific surveys from 2007 to 2010 off the EEZ of Costa Rica, Peru and Chile in an area, defined from 75°00′ W to 96°30′W and from 9°30′ N to 37°30′S, in the Eastern Pacific Ocean. The surveys were conducted with commercial vessels using jigging (Figure 1, Table 1). Statoliths were removed in the field and stored in 90% alcohol for further analyses. Detailed information of the samples is summarized in Table 1.

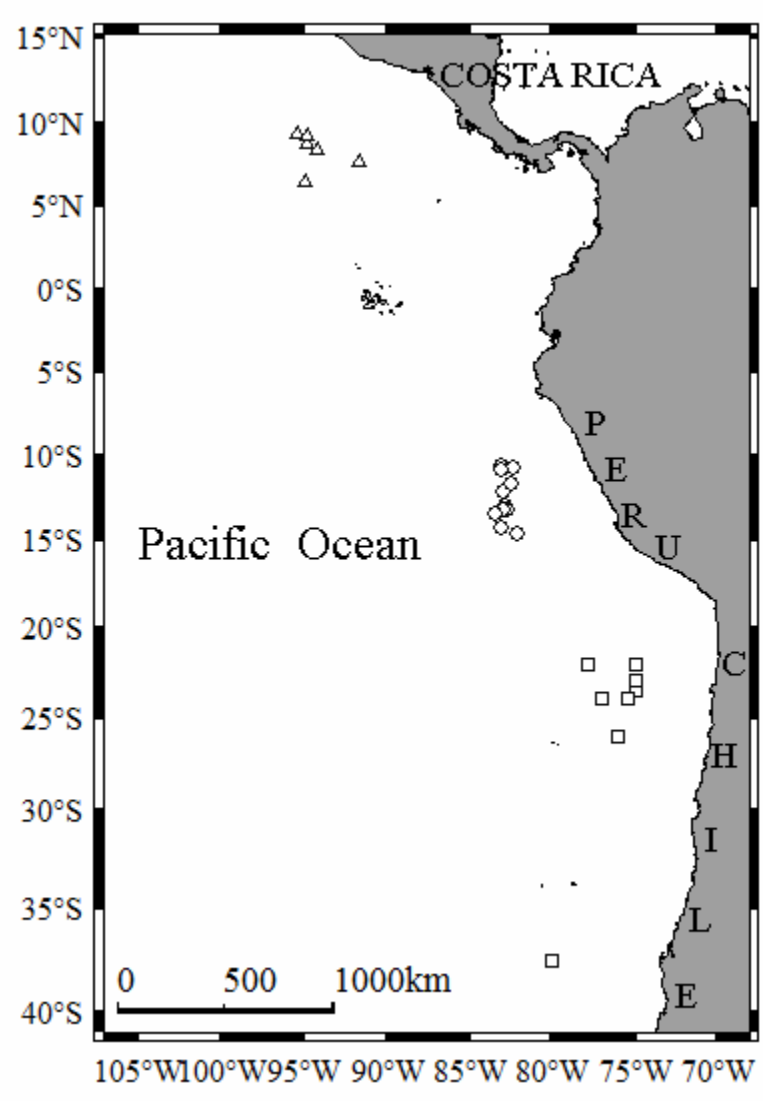


Figure 1 Sampling locations for *Dosidicus gigas* in the Eastern Pacific Ocean.

Table 1. Summary information of sampled *Dosidicus gigas* squid. ML: mantle length, BW: body weight, ♀: female, ♂: male. Dates are given as yyyy:mm:dd

| ID | Catch date | Location | Coordinates | ML (mm) | Sex | Maturity stage | Spot 1 age (days) | Spot 2 age (days) |
|---|---|---|---|---|---|---|---|---|
| 03 | 2009:08:17 | Costa Rica | 8°55′N, 94°55′W | 263 | ♂ | Mature | 0 | 18 |
| 30 | 2009:08:19 | Costa Rica | 8°35′N, 94°19′W | 259 | ♀ | Immature | 0 | 21 |
| SC10-3 | 2009:08:18 | Costa Rica | 9°21′N, 94°52′W | 348 | ♀ | Mature | 0 | 20 |
| SC10-10 | 2009:08:18 | Costa Rica | 9°21′N, 94°52′W | 285 | ♂ | Mature | 0 | 22 |
| 71 | 2009:08:09 | Costa Rica | 7°46′N, 91°48′W | 274 | ♀ | Immature | 0 | 24 |
| B10-2 | 2009:07:26 | Costa Rica | 9°30′N, 95°30′W | 271 | ♀ | Mature | 0 | 24 |
| SC07-11 | 2009:08:15 | Costa Rica | 6°36′N, 95°02′W | 250 | ♀ | Mature | 0 | 23 |
| SC10-21 | 2009:08:18 | Costa Rica | 9°21′N, 94°52′W | 310 | ♂ | Mature | 0 | 21 |
| 72 | 2009:08:09 | Costa Rica | 7°46′N, 96°30′W | 295 | ♂ | Mature | 0 | 19 |
| D8-8 | 2009:07:29 | Costa Rica | 8°30′N, 94°52′W | 374 | ♀ | Mature | 0 | 25 |
| 61b | 2008:09:20 | Peru | 10°32′S, 83°14′W | 258 | ♀ | Immature | 0 | 26 |
| 70b | 2008:09:20 | Peru | 10°32′S, 83°14′W | 291 | ♀ | Immature | 0 | 26 |
| 124b | 2008:09:13 | Peru | 10°39′S, 82°29′W | 278 | ♀ | Immature | 0 | 27 |
| 140b | 2008:09:13 | Peru | 10°39′S, 82°29′W | 275 | ♀ | Immature | 0 | 25 |
| A208 | 2009:09:13 | Peru | 11°12′S, 83°17′W | 311 | ♀ | Immature | 0 | 24 |
| A77 | 2009:10:01 | Peru | 10°59′S, 82°41′W | 294 | ♂ | Immature | 0 | 22 |
| C0923 | 2009:09:23 | Peru | 10°45′S, 83°10′W | 989 | ♀ | Mature | 0 | 28 |
| D107 | 2008:02:11 | Peru | 13°22′S, 83°28′W | 383 | ♂ | Mature | 0 | 23 |
| D12 | 2008:01:10 | Peru | 12°54′S, 82°56′W | 454 | ♀ | Mature | 0 | 27 |
| D42 | 2008:01:21 | Peru | 13°06′S, 82°46′W | 343 | ♂ | Immature | 0 | 23 |
| D94 | 2008:02:04 | Peru | 13°03′S, 83°04′W | 325 | ♀ | Immature | 0 | 25 |
| E176 | 2008:12:14 | Peru | 13°20′S, 83°29′W | 275 | ♀ | Immature | 0 | 24 |
| E202 | 2008:11:30 | Peru | 11°54′S, 83°04′W | 303 | ♀ | Immature | 0 | 27 |
| E32 | 2009:01:25 | Peru | 12°45′S, 83°45′W | 434 | ♀ | Mature | 0 | 23 |
| E54 | 2008:11:24 | Peru | 12°00′S, 83°05′W | 302 | ♀ | Immature | 0 | 22 |
| G198 | 2010:01:16 | Peru | 14º43´S, 83º33´W | 353 | ♀ | Mature | 0 | 28 |
| G267 | 210:03:10 | Peru | 16º27´S, 79º26´W | 435 | ♀ | Immature | 0 | 29 |
| G288 | 2009:12:20 | Peru | 15º02´S, 80º35´W | 333 | ♂ | Immature | 0 | 24 |
| G422 | 2009:11:15 | Peru | 11°29′S, 82°31′W | 450 | ♀ | Immature | 0 | 25 |
| G54 | 2010:02:05 | Peru | 14º07´S, 83º10´W | 403 | ♀ | Immature | 0 | 26 |
| K154 | 2010:10:25 | Peru | 16º07´S, 82º14´W | 405 | ♀ | Immature | 0 | 27 |

| | | | | | | | | |
|---|---|---|---|---|---|---|---|---|
| K18 | 2010:06:15 | Peru | 16º25´S, 80º16´W | 243 | ♂ | Immature | 0 | 23 |
| K203 | 2010:08:10 | Peru | 10º52´S, 81º55´W | 223 | ♀ | Immature | 0 | 24 |
| K228 | 2010:11:30 | Peru | 15º39´S, 81º03´W | 502 | ♀ | Immature | 0 | 28 |
| K242 | 2010:11:10: | Peru | 14°31′S, 82°09′W | 359 | ♀ | Mature | 0 | 26 |
| K80 | 2010:06:20 | Peru | 15°52′S, 79°49′W | 529 | ♀ | Mature | 0 | 27 |
| 61a | 2008:05:01 | Chile | 23°00′S, 75°00′W | 381 | ♀ | Immature | 0 | 28 |
| 88a | 2008:05:07 | Chile | 22°00′S, 77°50′W | 449 | ♂ | Immature | 0 | 24 |
| 294a | 2008:05:12 | Chile | 22°00′S, 75°00′W | 391 | ♀ | Immature | 0 | 28 |
| 301a | 2008:05:12 | Chile | 22°00′S, 75°00′W | 401 | ♀ | Immature | 0 | 26 |
| 316a | 2008:05:12 | Chile | 23°00′S, 75°00′W | 341 | ♂ | Immature | 0 | 23 |
| 321a | 2008:05:09 | Chile | 24°00′S, 75°30′W | 372 | ♀ | Immature | 0 | 25 |
| 164b | 2008:05:12 | Chile | 22°00′S, 75°00′W | 402 | ♀ | Immature | 0 | 29 |
| 6b | 2007:01:20 | Chile | 24°00′S, 77°00′W | 391 | ♀ | Immature | 0 | 30 |
| 23b | 2007:01:21 | Chile | 26°00′S, 76°00′W | 425 | ♀ | Immature | 0 | 29 |
| 35b | 2007:01:25 | Chile | 37°30′S, 80°00′W | 368 | ♀ | Immature | 0 | 27 |
| 38b | 2007:01:25 | Chile | 37°30′S, 80°00′W | 309 | ♀ | Immature | 0 | 27 |
| 49b | 2008:05:14 | Chile | 21°00′S, 75°00′W | 373 | ♂ | Immature | 0 | 25 |
| 69b | 2008:05:01 | Chile | 23°00′S, 75°00′W | 361 | ♂ | Immature | 0 | 24 |
| 75b | 2008:05:07 | Chile | 22°00′S, 77°50′W | 517 | ♀ | Immature | 0 | 25 |
| F91 | 2010:06:17 | Chile | 26°41S, 75°29′W | 493 | ⚲ | Immature | 0 | 26 |
| G173 | 2010:05:15 | Chile | 28°27S, 75°49′W | 490 | ⚲ | Immature | 0 | 25 |
| G561 | 2010:04:30 | Chile | 27°48S, 75°31′W | 406 | ♂ | Immature | 0 | 24 |
| L210 | 2007:06:09 | Chile | 29°30S, 76°30′W | 395 | ⚲ | Immature | 0 | 29 |
| L216 | 2007:06:10 | Chile | 28°58S, 77°18′W | 390 | ♂ | Mature | 0 | 22 |
| L241 | 2007:06:11 | Chile | 27°00S, 76°00′W | 454 | ⚲ | Immature | 0 | 29 |
| M11 | 2008:02:24 | Chile | 21°34S,81°21′W | 553 | ⚲ | Mature | 0 | 28 |
| M14 | 2008:02:24 | Chile | 21°34S,81°21′W | 531 | ⚲ | Mature | 0 | 27 |
| SB12 | 2010:06:05 | Chile | 28°45S, 76°14′W | 426 | ⚲ | Immature | 0 | 27 |

## *Sample preparation*

Each individual statolith was ground on a longitudinal plane with 3M® commercial waterproof sandpaper (600, 1200, 2000 grit) until the nucleus was exposed. It was then turned over and ground to the nucleus from the other side. Eventually, the ground statolith was polished with 0.3μm alumina powder for further elemental signature analyses.

## *Elemental signatures analysis*

To minimize the interference from contaminants, the ground statolith sections were rinsed in MillIQ water (resistivity > 18 Ω) for 5 minutes and air dried in a Class-100 laminar flow bench prior to trace element analysis. The first sampling spot was within N and the second sampling spot was placed in the periphery of PN, and the age of each spot were estimated assuming the growth increments deposit daily. Fourteen elemental signatures ($^{7}$Li, $^{23}$Na, $^{24}$Mg, $^{39}$K, $^{43}$Ca, $^{55}$Mn, $^{59}$Co, $^{60}$Ni, $^{63}$Cu, $^{66}$Zn, $^{88}$Sr, $^{137}$Ba, $^{208}$Pb, $^{238}$U) were determined by LA-ICP-MS at the State Key Laboratory of Geological Processes and Mineral Resources, China University of Geosciences, using a 193 nm frequency-quadrupled ArF exciter laser coupled with Agilent 7500a. Ablation parameters in the analyses included spot size of 24 μm, and laser pulse of 5 Hz. Helium (0.7l $min^{-1}$) was used as a sample gas in the ablation cell and Argon (0.8l $min^{-1}$) was subsequently added to the gas flow. Every spot in the statolith was ablated for 20 s to determine the fourteen elements. Element concentrations were expressed as ratios to Ca in order to standardize the variation in the material ablated.

## *Statistical analysis*

In order to examine the spatial variability of the elemental signatures in the embryonic and paralaval statoliths, univariate and multivariate analyses of variance (ANOVA and MANOVA respectively) were performed. Both stepwise discriminant analysis (SDA) and principal component analysis (PCA) were used to examine the difference of elemental signatures between squid in the northern and southern hemisphere. SDA was also used to investigate the differences in multivariate elemental signatures among sampling locations. Mean scores and 95% confidence ellipses of the first two functions in the SDA were calculated. A jackknife reclassification procedure, also referred to as leave-one-out cross-validation, was used to determine the rates of successful classification of squid from different locations. The 95% confidence ellipses were calculated using R 2.13.1, and other statistical

analyses were performed with SPSS 19.0.

## 3. RESULTS

Two spots were place into N and PN to measure embroic and paralaval statolith elemental signatures. By counting growth increment, the age of spot within N are zero for all of samples, and the age of spot in the periphery of PN are from 18 to 25, 22 to 29 and 22 to 30 for the samples from Costa Rcia, Peru and Chile, respectively.

### *Ontogenetic signature difference*

Detected signature concentrations were expressed as their ratios to Ca which is the most abundant signature in the *D. gigas* statoliths with an almost constant value. Sr and Na are the two most abundant signatures besides Ca in the *D. gigas* statoliths, with concentrations over 10 mmol $mol^{-1}$, which is almost three orders of magnitude higher than that for other signatures including K, Mg, Ba, Zn, Mn, Cu, Ni, Li, Co, Pb, U, etc (Table 2). All measured signatures were significantly different between embryonic and paralarval statoliths (ANOVA, $P < 0.05$), except for Sr, Ba and Pb (ANOVA, $P > 0.05$), with Li, Na, Mg, Mn, Cu, Zn and U showing highly significant differences (ANOVA, $P < 0.01$). Mg, K, Mn, Co, Ni, Cu, Zn and U in embryonic statoliths were significantly higher, but Li and Na were significantly lower than those in paralarval statoliths (Table 2).

Table 2. Analysis of variance of signatures in the embryonic and paralarval statoliths (N and PN) for *Dosidicus gigas*. * implies significant difference.

| Element/Ca | Embryonic statolith | | Paralarval statolith | | F | p |
|---|---|---|---|---|---|---|
| | Range | Mean±Std | Range | Mean±Std | | |
| Li/Ca(μmol $mol^{-1}$) | 0.82-3.62 | 1.84±0.49 | 1.23-5.80 | 2.28±0.65 | 17.638 | 0.000* |
| Na/Ca(mmol $mol^{-1}$) | 8.74-13.3 | 10.6±1.12 | 9.12-13.9 | 11.3±1.15 | 13.885 | 0.000* |
| Mg/Ca(μmol $mol^{-1}$) | 80-1235 | 415±271 | 74-484 | 210±86 | 30.563 | 0.000* |
| K/Ca(μmol $mol^{-1}$) | 87-1360 | 468±237 | 56-971 | 365±194 | 6.631 | 0.011* |
| Mn/Ca(μmol $mol^{-1}$) | 0-21.8 | 7.66±4.79 | 0-15.1 | 3.85±2.60 | 28.816 | 0.000* |
| Co/Ca(μmol $mol^{-1}$) | 0-0.87 | 0.16±0.19 | 0-0.78 | 0.10±0.16 | 4.039 | 0.047* |
| Ni/Ca(μmol $mol^{-1}$) | 0-16.1 | 2.53±3.51 | 0-7.67 | 1.25±1.98 | 5.913 | 0.017* |
| Cu/Ca(μmol $mol^{-1}$) | 0-23.6 | 2.61±4.21 | 0-7.19 | 0.98±1.20 | 8.101 | 0.005* |
| Zn/Ca(μmol $mol^{-1}$) | 0-136 | 15.3±26.6 | 0-24.3 | 3.66±4.52 | 10.945 | 0.001* |
| Sr/Ca(mmol $mol^{-1}$) | 13.9-18.8 | 16.3±1.13 | 13.0-17.8 | 15.9±1.03 | 3.852 | 0.052 |
| Ba/Ca(μmol $mol^{-1}$) | 8.75-56.4 | 17.3±9.42 | 8.56-42.8 | 14.7±7.81 | 2.536 | 0.114 |
| Pb/Ca(μmol $mol^{-1}$) | 0-7.94 | 0.47±1.17 | 0-2.65 | 0.17±0.37 | 3.514 | 0.063 |
| U/Ca(μmol $mol^{-1}$) | 0-0.24 | 0.037±0.042 | 0-0.07 | 0.018±0.016 | 9.840 | 0.002* |

### *Geographic variation in signatures*

Most of the detected elemental signatures within the embryonic statoliths were found to have no significant difference, but Na and Ba had a significant difference among the three regions (Table 3, ANOVA, $P < 0.01$). By contrast, for paralarval statoliths, only Zn and Ba had a significant difference among the three regions (Table 3, ANOVA, $P < 0.01$). Besides, ANOVA also showed that Ba within the embryonic and paralarval statoliths from Peru were both similar with Chile, but significantly lower than those in Costa Rica (Table 4). The values of Mg/Ca and Mn/Ca both in the embryonic and paralarval statoliths from Costa Rica were the highest and those from Chile were the lowest (Table 4).

Table 3 Analysis of variance comparing elemental signature concentrations within embryonic and paralarval statoliths for *D. gigas* among the three regions. * implies significant difference.

| Signature | Embryonic statolith | | | | Paralarval statolith | | | |
|---|---|---|---|---|---|---|---|---|
| | MS | | F | P | MS | | F | P |
| | Regions | Error | | | Regions | Error | | |
| Li/Ca | 0.224 | 0.240 | 0.935 | 0.399 | 0.506 | 0.416 | 1.215 | 0.304 |
| Na/Ca | 4.623 | 1.127 | 4.102 | 0.022* | 1.503 | 1.320 | 1.139 | 0.327 |
| Mg/Ca | 203425 | 68701 | 2.961 | 0.060 | 10267 | 7266 | 1.413 | 0.252 |
| K/Ca | 30265 | 57320 | 0.528 | 0.593 | 33226 | 37929 | 0.876 | 0.422 |
| Mn/Ca | 55.969 | 21.761 | 2.572 | 0.085 | 10.639 | 6.625 | 1.606 | 0.210 |
| Co/Ca | 0.042 | 0.035 | 1.186 | 0.314 | 0.017 | 0.026 | 0.659 | 0.521 |
| Ni/Ca | 1.184 | 12.731 | 0.093 | 0.911 | 0.225 | 4.018 | 0.056 | 0.946 |
| Cu/Ca | 11.034 | 17.941 | 0.615 | 0.544 | 0.124 | 1.494 | 0.083 | 0.920 |
| Zn/Ca | 250.567 | 726.281 | 0.345 | 0.710 | 98.296 | 17.685 | 5.558 | 0.006* |
| Sr/Ca | 0.746 | 1.291 | 0.578 | 0.564 | 1.337 | 1.044 | 1.281 | 0.286 |
| Ba/Ca | 730.554 | 65.798 | 11.103 | 0.000* | 564 | 43.078 | 13.101 | 0.000* |
| Pb/Ca | 1.603 | 1.350 | 1.187 | 0.313 | 0.058 | 0.142 | 0.409 | 0.666 |
| U/Ca | 0.003 | 0.002 | 1.718 | 0.189 | 0000 | 0.000 | 0.899 | 0.413 |

In the SDA of the multi-elemental signatures within embryonic statoliths, the results indicated that only Na, Mg and Ba made significant contributions to the determination of origins of samples (SDA, $P < 0.05$), and squid from different locations could be distinguished from each other using the first two functions, which explained 75.9% and 24.1% of the variations, respectively (Figure 2). However, for paralarval statoliths, only K, Zn and Ba were responsible for all the contributions to the classification (SDA, $P < 0.05$), with discriminant function 1 (DF1) explaining the most variations (Figure 2).

Table 4. Elemental signature concentrations within embryonic and paralarval statoliths for D. gigas from the three different regions

| Signature/Ca | Mean ± Std value of embryonic statolith | | | Mean ± Std value of paralarval statolith | | |
|---|---|---|---|---|---|---|
| | Costa Rica | Peru | Chile | Costa Rica | Peru | Chile |
| Li/Ca(μmol mol$^{-1}$) | 1.67±0.27 | 1.84±0.50 | 1.92±0.54 | 2.60±1.30 | 2.20±0.39 | 2.25±0.44 |
| Na/Ca(mmol mol$^{-1}$) | [a] 9.87±0.69 | [ab] 10.5±0.93 | [b]11.0±1.30 | 11.3±1.17 | 11.1±1.14 | 11.6±1.15 |
| Mg/Ca(μmol mol$^{-1}$) | 455±396 | 490±223 | 312±233 | 249±125 | 209±60.5 | 194±89.4 |
| K/Ca(μmol mol$^{-1}$) | 406±245 | 497±281 | 461±179 | 342±246 | 336±179 | 407±189 |
| Mn/Ca(μmol mol$^{-1}$) | 9.84±5.11 | 8.21±5.44 | 6.09±3.33 | 4.73±3.09 | 4.14±2.92 | 3.15±1.80 |
| Co/Ca(μmol mol$^{-1}$) | 0.11±0.06 | 0.14±0.15 | 0.21±0.25 | 0.080±0.050 | 0.080±010 | 0.13±0.23 |
| Ni/Ca(μmol mol$^{-1}$) | 2.93±2.51 | 2.53±3.53 | 2.35±3.96 | 1.26±1.74 | 1.34±2.11 | 1.15±2.00 |
| Cu/Ca(μmol mol$^{-1}$) | 1.37±1.01 | 3.12±4.56 | 2.57±4.66 | 1.06±0.73 | 0.91±0.89 | 1.03±1.64 |
| Zn/Ca(μmol mol$^{-1}$) | 18.3±37.3 | 12.0±10.8 | 17.7±33.9 | [a] 7.63±7.33 | [b] 3.20±3.68 | [b] 2.46±2.79 |
| Sr/Ca(mmol mol$^{-1}$) | 16.4±0.65 | 16.4±0.96 | 16.1±1.43 | 16.3±0.72 | 15.9±0.86 | 15.7±1.26 |
| Ba/Ca(μmol mol$^{-1}$) | [a] 28.3±16.2 | [b] 14.8±5.80 | [b] 15.3±4.69 | [a] 24.4±12.6 | [b] 12.4±3.98 | [b] 13.1±5.19 |
| Pb/Ca(μmol mol$^{-1}$) | 0.96±2.46 | 0.30±0.53 | 0.46±0.81 | 0.17±0.15 | 0.13±0.16 | 0.23±0.57 |
| U/Ca(μmol mol$^{-1}$) | 0.026±0.021 | 0.048±0.054 | 0.029±0.032 | 0.020±0.018 | 0.15±0.017 | 0.021±0.014 |

Std is standard deviation. The results from Tukey's HSD with significant difference ($P < 0.05$) indicated by letters (a, b)

Although there was considerable overlap, squid from different locations could be separated, with final cross-validated classification rates of 61% and 52.5% for embryonic and paralarval statoliths, respectively (Table 5, Figure 2). Overall, Ba contributed the greatest variation among the three sampling locations at the two functions, which can be seen from the values of the canonical coefficients (Table 6, Figure 2).

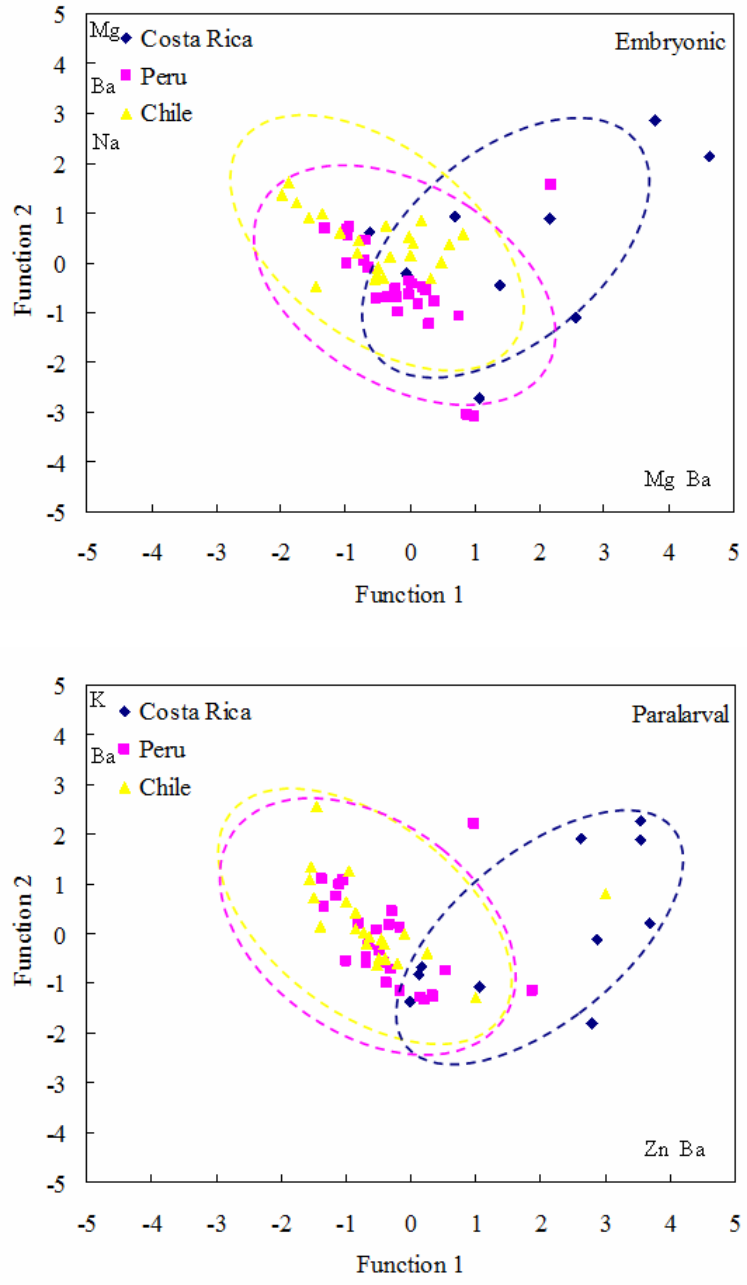


Figure 2 Discriminant function plots of embryonic and paralarval statolith to compare multi-elemental signatures among sampling locations using elements/Ca for *Dosidicus gigas*. Diamond: Costa Rica; Square: Peru; Triangle: Chile; Ellipses represents 95% confidence interval around centroids of each group.

Table 5. Cross-validated classification rate and values of Wilks'λ on the basis of discriminant function analysis scores of multi-elemental signatures within embryonic and paralarval statolith for *D. gigas* from different regions

| Statolith | Region | Cross-validated classification rate | | | |
|---|---|---|---|---|---|
| | | Costa Rica | Peru | Chile | Final |
| Embryonic | Costa Rica | 60.0% | 30.0% | 10.0% | 61.0% |
| | Peru | 3.8% | 65.4% | 30.8% | |
| | Chile | 8.7% | 34.8% | 56.5% | |
| Paralarval | Costa Rica | 60.0% | 40.0% | 0.0% | 52.5% |
| | Peru | 7.7% | 53.8% | 38.5% | |
| | Chile | 8.7% | 43.5% | 47.8% | |

Table 6. Standardized canonical DF coefficients for Function 1 and Function 2 for each signature/Ca used in discriminant function analysis for *D. gigas* among the three sampling regions. Coefficients represent the relative contribution of each signature/Ca to each DF.

| Statolith | Signature | DF1 | DF2 |
|---|---|---|---|
| Embryonic | Na/Ca | -0.625 | 0.508 |
| | Mg/Ca | 0.300 | 0.864 |
| | Ba/Ca | 0.808 | 0.541 |
| Paralarval | K/Ca | -0.554 | 0.821 |
| | Zn/Ca | 0.597 | -.329 |
| | Ba/Ca | 0.961 | 0.302 |

## *Hemispherical variation in signatures*

Multi-elemental signatures within embryonic and paralarval statoliths from the northern (Costa Rica) and southern hemisphere (Peru and Chile) used in the SDA showed that the final correct cross-validated classification rates were 84.7% and 88.1%, respectively, with a total Wilks'λ value of 0.665 and 0.529 ($P < 0.001$) (Table 7). This suggested that elemental signatures have significant hemispherical differences, in spite of considerable overlaps as shown by the PCA scatter-plots (Figure 3).

Table 7. Cross-validated classification rate and values of Wilks'λ on the basis of discriminant function analysis scores of multi-elemental signatures within embryonic and paralarval statolith for *D. gigas* from different hemisphere

| Statolith | Hemisphere | Cross-validated classification rate | | | Wilks'λ | p |
|---|---|---|---|---|---|---|
| | | Northern | Southern | Final | | |
| Embryonic | Northern | 60.0% | 40.0% | 84.7% | 0.655 | 0.000 |
| | Southern | 10.2% | 89.8% | | | |
| Paralarval | Northern | 70.0% | 30.0% | 88.1% | 0.529 | 0.000 |
| | Southern | 8.2% | 91.8% | | | |

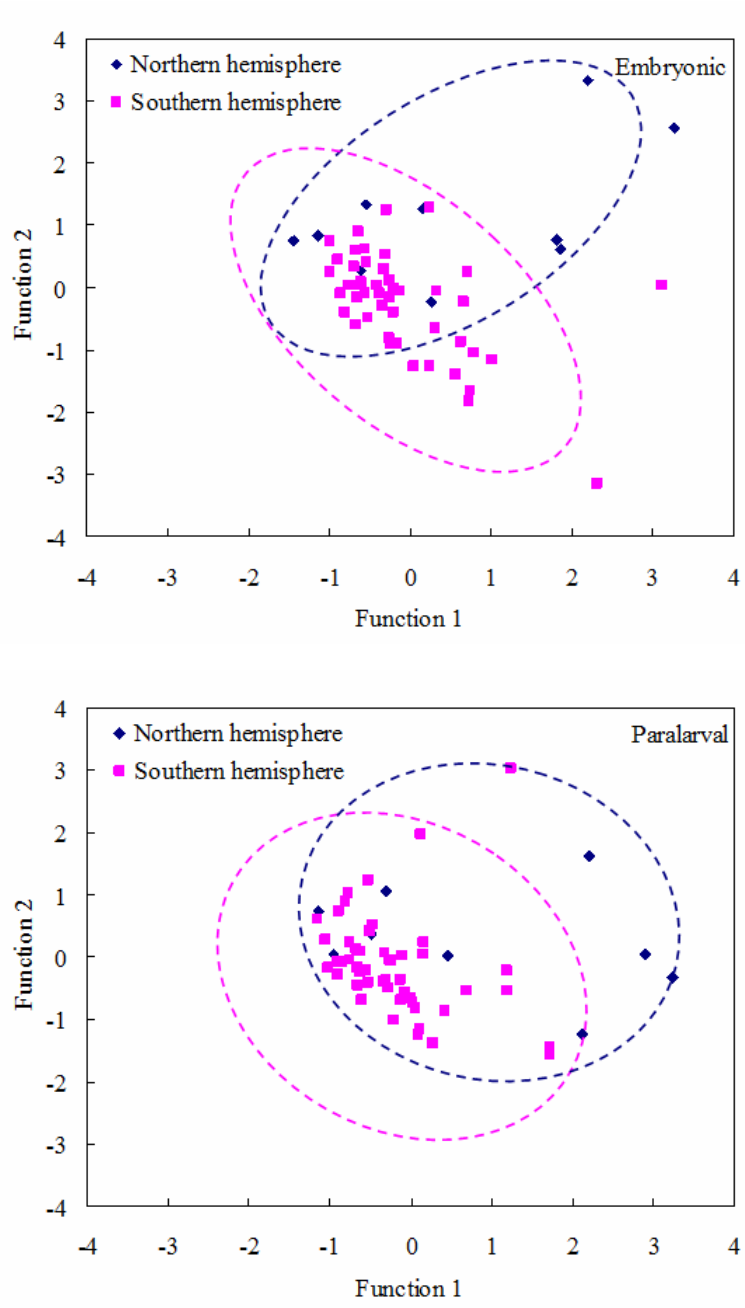


Figure 3 Factorial Score plots of embryonic and paralarval statolith to compare multi-elemental signatures among sampling hemisphere using elements/Ca for *Dosidicus gigas*.

## 4. Conclusion

In conclusion, all measured signatures were significantly different between embryonic and paralarval statoliths, except for Sr, Ba and Pb. Na and Ba within embryonic statoliths and Zn and Ba within paralarval statoliths where significant differences were found among the three regions. A significantly higher Ba/Ca ratio in the statoliths collected from Costa Rica was found, compared with those from Peru

and Chile, which might result from the prevalence of strong upwelling in Costa Rica, and a similar Ba/Ca between Peru and Chile might be influenced by the same current that is Humboldt. Elemental signatures in embryonic statoliths were considered to be a better natural tag than those in paralarval statoliths, although both of them could be used as a proxy for distinguishing different groups. The paralarvae of the same populations followed different dispersal trajectories, which might be responsible for their differences.

We prefer to believe that the northern (Costa Rica) and southern (Peru and Chile) group potentially have different natal origins and migration patterns. The northern population was putative spawning adjacent to the Costa Rica Dome, and the special Equatorial Counter Current meant that the paralarvae remained in the spawning ground for food. In contrast, the southern population might spawn in the coastal waters off northern Peru, and the paralarvae would be carried northward rather than stay at the birth place for nursery. Overall, the jumbo squid life cycle, especially at early ontogeny stage, is susceptible to variation of oceanography, particularly the ENSO. For instance, during normal and cold years, intensive offshore transport carry paralarvae far away from the coast into the large open sea area, but during warm years, a weak current retains the paralarvae near the shelf. Therefore, considering higher plasticity of the squid and specificity of the study region, it is important for future studies to access how and where the squid might move as the climate change.

## REFERENCES

Arkhipkin, A.I. (2005) Statolith as ‘balck boxes’(life recorders) in squid. *Mar. Freshw. Res.* 56:573-583.

Arkhipkin, A.I. Campana, S.E. FitzGerald, J. and Thorrold, S.R. (2004) Spatial and temporal variation in elemental signatures of statoliths from the Patagonian longfin squid (*Loligo gahi*). *Can. J. Fish. Aqua. Sci.* 61:1212-1224.

Becker, B.J. Fodrie, F.J. McMillan, P.A. and Levin, L.A. (2005) Spatial and temporal variation in trace elemental fingerprints of mytilid mussel shells: A precursor to invertebrate larval tracking. *Limnol. Oceanogr.* 50(1):48-61.

Campana, S.E. (1999) Chemistry and composition of fish otoliths: pathways, mechanisms and applications. *Mar. Ecol. Prog. Ser.* 188:263-297.

Chen, X.J. and Zhao, X.H. (2006) Preliminary study on the catch distribution of

*Dosidicus gigas* and its relationship with sea surface temperature in the offshore waters of Peru. *J. ShangH. Fish. Univ.* 15(1):65-70.

Cherel, Y. and Hobson. K. (2005) Stable isotopes, beaks and predators: a new tool to study the trophic ecology of cephalopods, including giant and colossal squids. *Proc. R. Soc. B.* 272:1601-1607.

Clarke, R. and Paliza, O. (2000) The Humboldt current squid *Dosidicus gigas* (Orbigny, 1835). *Rev. Biol. Mar. Oceanogr.* 35:1-38.

Doubleday, Z.A. Pecl, G.T. Semmens, J.M. and Danyushevsky, L. (2008) Stylet elemental signatures indicate population structure in a holobenthic octopus species, *Octopus pallidus*. *Mar. Ecol. Prog. Ser.* 371:1-10.

Durholtz, M.D. Lipinski, M.R. Przybylowicz, W.J. and Mesjasz-Przybylowicz, J. (1997) Nuclear microprobe mapping of statoliths of Chokka Squid *Loligo vulgaris reynaudii* d'Orbigny, 1845. *Biol. Bull.* 193:125-140.

Forrester, G.E. and Swearer, S.E. (2002) Trace elements in otoliths indicate the use of open-coast verses bay nursery habitats by juvenile California halibut. *Mar. Ecol. Prog. Ser.* 241:201-213.

Gillanders, B.M. (2002) Connectivity between juvenile and adult fish populations: do adults remain near their recruitment estuaries? *Mar. Ecol. Prog. Ser.* 240:215-223.

Hamer, P.A. Jenkins, G.P. and Gillanders, B.M. (2005) Chemical tags in otoliths indicate the importance of local and distant settlement areas to populations of a temperate sparid, *Pagrus auratus*. *Can. J. Fish. Aquat. Sci.* 62:623-630.

Ichii, T. Mahapatra, K. Watanabe, T. Yatsu, A. Inagake, D. and Okada, Y. (2002) Occurrence of jumbo fying squid *Dosidicus gigas* aggregations associated with the countercurrent ridge off the Costa Rica Dome during 1997 El Niño and 1999 La Niña. *Mar. Ecol. Prog. Ser.* 231:151-166.

Ikeda, Y. Arai, N. Kidokoro, H. and Sakamoto, W. (2003) Strontium:calcium ratios in statoliths of Japanese common squid *Todarodes pacificus* (Cephalopoda: Ommastrephidae) as indicators of migratory behaviour. *Mar. Ecol. Progr. Ser.* 251:169-179.

Ikeda, Y. Yatsu, A. Arai, N. and Sakamoto, W. (2002) Concentration of statolith trace elements in the jumbo flying squid during El Niño and non-El Niño years in the eastern Pacific. *J. Mar. Biol. Assoc. UK.* 82:863-866.

Kalish, J.M. (1990) Use of otolith microchemistry to distinguish the progeny of

sympatric anadromous and non-anadromous salmonids. *Fish. Bull. US.* 88:657-666.

Keyl. F. Argüelles, J. Mariátegui, L. Tafur, R. Wolff, M. and Yamashiro, C. (2008) A hypothesis on range expansion and spatio-temporal shifts in size-at-maturity of jum

Liu B L, Chen X J, Lu H J, Chen Y, and Qian W G (2010) Fishery biology of the jumbo squid *Dosidicus gigas* off Exclusive Economic Zone of Chilean waters. Sci Mar 74: 687-695

Liu, B.L. Chen, X.J. Chen, Y. Lu, H.J. and Qian, W.G. (2011) Trace elements in the statoliths of jumbo flying squid off the Exclusive Economic Zones of Chile and Peru. *Mar. Ecol. Prog. Ser.* 429:93-101.

Morales-Bojórquez, E. Cisneros-Mata, M.A. Nevárez-Martínez, M.O. and Hernández-Herrera, A. (2001) Review of stock assment and fishry biology of *Dosidicus gigas* in the Gulf of California, Mexico. *Fish. Res.* 54:83-84.

Nesis, K.N. (1983) *Dosidicus gigas*. In: P.R. Boyle (ed) Cephalopod life cycles, Vol 1. Species accounts. Academic Press, London, pp. 216-231.

Nevárez-Martínez, M.O. Hernández-Herrera, A. Morales-Bojórquez, E. Balmori-Ramírez, A. Cisneros-Mata, M.A. and Morales-Azpeitia, R. (2000) Biomass and distribution of the jumbo squid (*Dosidicus gigas*; d'Orbigny, 1835) in the Gulf of California, Mexico. *Fish. Res.* 49:129-140.

Nigmatullin, Ch. M. Nesis, K.N. and Arkhipkin, A.I. (2001) A review of the biology of the jumbo squid *Dosidicus gigas* (Cephalopoda: Ommastrephidae). *Fish. Res.* 54:9-19.

Rosas-Luis, R. Salinas-Zavala, C.A. Koch, V. Del Monte, L. P. and Morales-Zárate, M. V. (2008) Importance of jumbo squid *Dosidicus gigas* (Orbigny, 1835) in the pelagic ecosystem of the central Gulf of California. *Ecol. Model.* 218:149-161.

Rocha, F. and Vega, M. (2003) Overview of cephalopod fisheries in Chilean waters. *Fish. Res.* 60:151-159.

Sandoval-Castellanos, E. Uribe-Alcocer, M. and Díaz-Jaimes, P. (2007) Population genetic structure of jumbo squid (*Dosidicus gigas*) evaluated by RAPD analysis. *Fish. Res.* 83:113-118.

Taipe, A. Yamashiro, C. Mariategui, L. Rojas, P. and Roque, C. (2001) Distribution and concentration of jumbo flying squid (*Dosidicus gigas*) off the Peruvian coast between 1991 and 1999. *Fish. Res.* 54: 21-32.

Thorrold, S.R. Latkoczy, C. Swart, P.K. and Jones, C.S. (2001) Natal homing in a

marine fish metapopulation. *Sci.* 291:297-299.

Waluda, C.M. Yamashiro, C. Elvidge, C.D. Hobson, V.R. and Rodhouse, P.G. (2004a) Quantifying light-fshing for *Dosidicus gigas* in the Eastern Pacific using satellite remote sensing. *Remote Sens Environ.* 91:129-133.

Waluda, C.M. Yamashiro, C. and Rodhouse, P.G. (2006) Influence of the ENSO cycle on the light-fishery for *Dosidicus gigas* in the Peru Current: an analysis of remotely sensed data. *Fish. Res.* 79:56-63.

Warner, R.R. Hamilton, S.L. Sheehy, M.S. Zeidberg, L.D. Brady, B.C. and Caselle, J.E. (2009) Geographic variation in natal and early larval trace-elemental signatures in the statoliths of the market squid *Doryteuthis* (formerly *Loligo*) *opalescens*. *Mar. Ecol. Prog. Ser.* 379:109-121.

Yatsu, A. Mochioka, N. Morishita, K. and Toh, H. (1998) Strontium:calcium ratios in statoliths of the neon flying squid, *Ommastrephes bartrami* (Cephalopoda), in the North Pacific Ocean. *Mar. Biol.* 131:275-282.

Zacherl, D.C. (2005) Spatial and temporal variation in statolith and protoconch trace elements as natural tags to track larval dispersal. *Mar. Ecol. Prog. Ser.* 290:145-163.

Zacherl, D.C. Manríquez, P.H. Paradis, G.L. Day, R.W. Castilla, J.C. Warner, R. R. Lea, D.W. and Gaines, S.D. (2003) Trace elemental fingerprinting of gastropod statoliths to study larval dispersal trajectories. *Mar. Ecol. Prog. Ser.* 248:297-303.

Zeidberg, L.D. and Robison, B.H. (2007) Invasive range expansion by the Humboldt squid, *Dosidicus gigas*, in the eastern North Pacific. *Proc. Natl. Acad. Sci. US.* 104:12948-12950

Zumholz, K. Hansteen, T.H. Klügel, A. and Piatkowski, U. (2006) Food effects on statolith composition of the common cuttlefish (*Sepia officinalis*). *Mar. Biol.* 150:237-244.

Zumholz, K. Klügel, A. Hansteen, T.H. and Piatkowski, U. (2007) Statolith microchemistry traces environmental history of the boreoatlantic armhook squid *Gonatus fabricii*. *Mar. Ecol. Prog.* Ser. 333:195-204.

Zúñiga, M.J. Cubillos, L.A. and Ibáñez, C. (2008) A regular pattern of periodicity in the monthly catch of jumbo squid (*Dosidicus gigas*) along the Chilean coast (2002-2005). *Cien. Mar.* 34:91-99